RESEARCH ARTICLE

Macromolecular Chemistry and Physics
www.mcp-journal.de

Solid Polymer Electrolytes Based on Phosphonate and Cyclocarbonate Units for Safer Full Solid State Lithium Metal Batteries

*Benoît Notredame, Fernand Gauthy, Vincent Finsy, and Jean-François Gohy**

Solid-state polymer electrolytes are key components for future batteries with higher energy density as well as increased safety and processability. In this context, a solid polymer electrolyte is developed from statistical copolymers containing flame-retardant phosphonate units and ion-conductive cyclocarbonate moieties mixed with lithium salts. Ionic conductivity measured at room temperature for those copolymers (≈10^{-5} S cm^{-1}) are in the same range as typical solid polymeric electrolytes not based on poly(ethylene oxide). Moreover, those copolymers electrolytes are stable in a wide electrochemical window (0.5 – 4.5 V vs Li^+/Li) and at high temperature (>120 °C) and they lead to a better ionic conductivity than the corresponding homopolymer blends of a similar composition, which is explained by a better lithium salt solubility and better-defined ion-conduction pathways in case of the copolymer. Finally, it has demonstrated the possibility to have fire-retardant properties afforded by phosphonate groups in copolymers without impacting the ionic conductivity.

1. Introduction

The use of batteries is spreading in all different parts of our society, e.g., small electronic equipments, smartphones, laptops, and electric cars. This last sector is expected to grow up from 5.4 million units in 2018 to 440 million units in 2035, which will represent 42.5% of total car inventory worldwide.[1] To fulfill the future sales of electric cars, the production of batteries is changing: first to supply the huge need of raw materials needed in the car sector,[2] then to fit the new customer expectations in terms of range and safety.[3,4] Nowadays, batteries are mainly using the lithium-ion technology with its inherent drawbacks including the use of organic solvents-based electrolytes, the impossibility to reach a high voltage (>4.5 V vs Li^+/Li) and the need to significantly improve the energy density.[5] To face these issues, the technology of all solid-state lithium metal batteries is currently being investigated. Indeed, the utilization of a lithium metal anode is the most obvious way to increase the energy density since it offers the highest specific theoretical capacity at the anode side (3860 mAh g^{-1}).[6] However, due to the high reactivity of lithium metal and the need to create a stable solid electrolyte interface (SEI), this new generation of batteries requires new innovations regarding the electrolytes. In this respect, solid polymer electrolytes (SPEs) are interesting candidates.[7] The ideal SPE must be compatible with both lithium metal anodes and with high voltage cathode materials (until 5 V vs Li^+/Li)[8,9] and with all the materials contained in both electrodes.[10,11] Its ionic conductivity at room temperature must be beyond 0.1 mS cm^{-1} in order to allow the battery to deliver an adequate power density compared to liquid electrolyte.[12] Last, it should offer good mechanical properties (modulus > 6 GPa) to avoid dendrites growth, and be easily processable.[13–15]

Nowadays, the most investigated SPEs are poly(ethylene oxide) (PEO)-based polymers loaded with lithium salts[16,17] which have been pioneered by Fenton et al.[18] PEO has been selected for its oxyethylene groups which show good solvation properties with a wide range of salts via interactions between their oxygen atoms with the lithium cations from the added lithium salt.[19] Usually, SPEs based on bare PEO show relatively low ionic conductivity, around 10^{-7} S cm^{-1} at room temperature,[20–23] due to a strong interaction between the lithium cations and the oxygen from ether groups as well as the high crystallinity of the polymer. The main mechanism explaining the mobility of lithium ions is the lithium-ion hopping between different polymer segments.[24–26] The most obvious way to increase the mobility of lithium ions is to increase the mobility of PEO segments by, e.g., increasing temperature,[24–26] adding additives acting as plasticizers,[27] or changing the architecture of the polymer by incorporating oligo(ethylene glycol) monomethyl ether methacrylate (OEGMA) units as side chains, for example.[28]

Another polymer family that shows growing interest is based on carbonate-containing polymers. In this respect, linear poly(ethylene carbonate)[29] and poly(propylene carbonate)[30] which are both stable until 4.5 V versus Li/Li^+ and lead, after

B. Notredame, J.-F. Gohy
Institute of Condensed Matter and Nanosciences (IMCN)
Université catholique de Louvain
Place L. Pasteur 1, Louvain-la-Neuve 1348, Belgium
E-mail: jean-francois.gohy@uclouvain.be
F. Gauthy, V. Finsy
Solvay S.A. Solid State Battery Applicability Laboratory (SSBA)
Rue de Ransbeek 310, Brussels 1000, Belgium

The ORCID identification number(s) for the author(s) of this article can be found under https://doi.org/10.1002/macp.202200152

DOI: 10.1002/macp.202200152

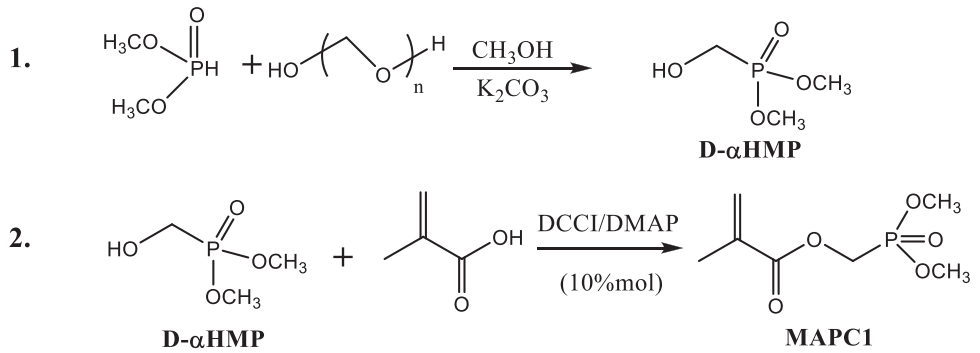

Scheme 1. Two-Step Synthesis of MAPC1.

lithium salt loading, to ionic conductivity ≈10^{-4} S cm^{-1} at room temperature have been considered. Moreover, carbonate-based SPEs supported on a cellulose matrix lead to better mechanical properties than PEO. Also, cyclic carbonates bearing monomers have been randomly copolymerized with butylacrylate[31] and vinylidene fluoride[32] leading, after salt loading, to ionic conductivity reaching 4.2 × 10^{-6} S cm^{-1} and 2 × 10^{-4} S cm^{-1} at room temperature, respectively. Nevertheless, those carbonate-based SPEs, such as PEO, are still flammable and may cause safety problems especially when lithium dendrites are formed in the lithium metal battery.[29]

Interestingly enough, phosphorus-containing organic compounds such as dimethyl methyl phosphonate[33] are often used in batteries as additives because of their fire-retardant characteristics.[34–36] Nevertheless, SPEs containing phosphonate moieties in their polymer structure have been hardly investigated. Zheng et al. studied different gel polymer electrolytes (GPEs) including a phosphonate-containing monomer for its nonflammable properties. Those GPEs were tested in sodium-ion batteries and showed ionic conductivity values around 10^{-3} S cm^{-1} at room temperature,[37–39] which are comparable to values obtained on nonflammable phosphonate-containing GPEs based on a poly(vinylidene fluoride-*co*-hexafluoropropylene) matrix.[40] Notwithstanding those previous reports, the use of phosphonate-based polymers for full solid-state lithium metal batteries has only been reported by Macarie's,[41] Gohy's,[42] Wang[43] and Mercerreyes's[44] groups to the best of our knowledge.

Based on those previous studies, we report here a novel phosphonate-containing SPE that combines the nonflammability of phosphonate moieties and the ionic conductivity of cyclocarbonate groups in an all-solid-state configuration. Moreover, we study the impact of each unit regarding the lithium salt dissociation and its incorporation in a statistical copolymer or in a blend of the corresponding homopolymers.

2. Experimental Section

2.1. Materials

All reactants have been purchased from Sigma Aldrich Company, except glycol-1,2-carbonate which was bought from Molbase Company. All of them were used as purchased, without purification except azobisisobutyronitrile which was recrystallized in methanol before use.

2.2. Synthesis of Poly(dimethyl(methacryloyloxy)methyl Phosphonate) (Poly(MAPC1))

The dimethyl(methacryloyloxy)methyl phosphonate (MAPC1) monomer synthesis has been carried out following the method previously reported by Loubat et al.[45] This synthesis was a two-step reaction (see **Scheme 1**) consisting first of the synthesis of dimethyl-*α*-hydroxymethylphosphonate (D-*α*HMP) obtained by reacting 20 g (0.18 mol) of dimethyl phosphite and 5.51 g (0.18 mol) of paraformaldehyde in 60 mL of methanol under reflux (80 °C) during 2 h with 1.24 g (8 mmol) of anhydrous potassium carbonate as a drying agent. The solution was then filtered, and methanol was evaporated to lead 24, 8 g of a colorless liquid with 98.4% yield and 86.5 wt.% purity (see Figure S1, Supporting Information, ^{1}H NMR spectrum). Then, 20 g (0.14 mol) of D-*α*HMP were mixed with 12,3 mL (0,14 mol) of methacrylic acid, cooled down in an ice bath, and 2.89 g (0.014 mol) of dicyclocarbodiimide (DCCI) were dropwise added followed by 1.71 g (0.014 mol) of N,N-dimethyl-4-aminopyridine (DMAP), which were both dissolved in 40 mL of chloroform. Finally, the reaction was stirred for 2 h at room temperature and then filtered. The colorless solution was then distilled under a high vacuum (<0.2 mbar) at 130 °C to obtain 28.3 g of the MAPC1 monomer, a colorless liquid with 97% yield and >99 wt.% purity (see Figure S2, Supporting Information, ^{1}H NMR spectrum).

The homopolymerization of MAPC1 was realized by free radical polymerization and consisted in mixing 2 g (9.6 mmol) of MAPC1 with 10.9 mg (0.07 mmol) of azobisisobutyronitrile (AIBN) in 7 mL of N,N dimethylformamide (DMF). This solution was submitted to three freeze-thaw cycles to eliminate all residual oxygen, then the solution was heated at 70 °C for 5 h, and the obtained polymer was precipitated in diethyl ether. Finally, the poly(MAPC1) homopolymer was dried under vacuum (<0.5 mbar) at 40 °C for at least 24 h.[46] The obtained polymer was characterized by an apparent $\bar{M}n$ of 61 × 10^3 g mol^{-1} and a dispersity of 1.94 (see Figure S3, Supporting Information size exclusion chromatography, SEC, eluogram).

2.3. Synthesis of Poly(2-oxo-1,3-dioxolan-4-yl)methyl Methacrylate) (Poly(MACyCB))

The synthesis of (2-Oxo-1,3-dioxolan-4-yl)methyl methacrylate (MACyCB) was performed following Yoshikawa et al.

Scheme 2. One-Step Synthesis of MACyCB.

methodology[47] (see **Scheme 2**). In order to eliminate moisture traces, the glassware was flamed under a vacuum. Then, 10 g of glycerol-1,2-carbonate (0084 mol) dissolved in 40 mL of dichloromethane (DCM) and 6.67 mL of triethylamine (0.092 mol) were mixed. After 30 min stirring in an ice bath, 6.73 mL (0.092 mol) of methacryloyl chloride were added drop by drop for 30 min. After 20 h of reaction at room temperature, the final product was recovered after rotary evaporation followed by two extractions with deionized water and one with a saturated NaCl solution and a final drying with anhydrous sodium sulfate. 14.85 g of a yellow liquid were finally obtained with 95% yield and >95 wt% purity (see Figure S4, Supporting Information, ^{1}H NMR spectrum).

The homopolymerization of MACyCB was carried out using the methodology described hereabove for MAPC1. The obtained poly(MACyCB) polymer is characterized by a $\bar{M}n$ of 67×10^3 g mol^{-1} and a dispersity of 2.60 (See Figure S5, Supporting Information SEC eluogram).

2.4. Copolymer Synthesis

Different ratios of comonomers were used to synthesize random copolymers of MAPC1 and MACyCB by free radical polymerization from 10 to 90 mol% of MAPC1 (= *X*) and 100-*X* mol% of MACyCB. All batches were prepared with a total comonomers amount of 4 g, 44.2 mg (0.23 mmol) of AIBN and 15 mL of DMF. The reaction medium was heated at 70 °C for 6 h and then the copolymer was recovered by precipitation in diethyl ether followed by vacuum evaporation of the remaining solvent at 40 °C.

2.5. Preparation of Solid Polymer Electrolytes (SPEs)

SPE membranes were obtained by a drop-casting method. Practically, 0.1 g of polymers were mixed with a given amount of lithium bis(trifluoromethanesulfonyl)imide (LiTFSI) in 1 mL of acetonitrile for 30 min to reach a complete dissolution. This solution was then cast on a 15.5 mm diameter stainless-steel (SS) disk (0.5 mm thickness) or in a poly(tetrafluoroethylene) (PTFE mold (40 mm diameter) drop by drop to cover the substrate surface completely. These substrates were then put in a vacuum oven (<5 mbar) at 40 °C for 24 h to remove the acetonitrile completely. All these steps were performed in a glovebox with <0.1 ppm O_2 and <0.1 ppm H_2O. SPE membranes were prepared either from copolymers or a mix of homopolymers with the same ratio of both comonomers (MAPC1 and MACyCB) to assess the influence of the polymer architecture. Furthermore, membranes with a different molar ratio between the repeating units involved in the polymer part and the LiTFSI were also prepared, from "repeating units":LiTFSI molar ratio of 5:1, 1:1, and 1:2. The ratio 5:1 means that there were 5 monomer units in the polymer chains for one Li^+ cation.

After complete solvent removal, a second SS disk was deposited on top to sandwich the SPE membrane between the two disks. To measure ionic conductivity, the samples were further sandwiched between two gold electrodes and sealed in an ITS (Intermediate Temperature System) cell to ensure an argon atmosphere during the measurement which leads to an Au|SS|SPE|SS|Au configuration. In the case of electrochemical stability tests, the SPE membrane cast on the first SS disk was mounted in a CR2025 coin cell with a lithium disk in contact with the top SPE membrane and another stainless disk to fill the cell. The whole assembly was pressed at 5 tons to seal it, leading to a Li|SPE|SS configuration. For DSC, TGA and flammable resistance, the SPE solution was cast in a PTFE mold and recovered as a free-standing film.

2.6. Characterization

2.6.1. Nuclear Magnetic Spectroscopy (NMR)

^{1}H NMR spectra were recorded on a 300 MHz Bruker Avance II using as solvent chloroform-d for monomers, DMF-d7 and acetonitrile-d3 for polymers.

2.6.2. Differential Scanning Calorimetry (DSC)

DSC measurements were carried out using a Mettler Toledo 823 calorimeter. Samples were prepared with different molar ratios of lithium salt (1:1 and 1:2, polymer:LiTFSI) and ≈10 mg were sealed in a 40 µl aluminum pan under a controlled atmosphere (<0.1 ppm O_2 and H_2O). An empty aluminum pan was used as a reference. The samples were first heated under nitrogen from −65 to 115 °C at a heating rate of 20 °C min^{-1} and this temperature was maintained for 1 min before cooling down to −65 °C and finally heating again to 115 °C to determine the glass transition temperature (T_g) of polymers, using the Stare software.

2.6.3. Thermogravimetric Analysis (TGA)

TGA was carried out using a Mettler Toledo TGA/DSC1 using the Stare software. Samples were prepared with different molar ratios of lithium salt (LiTFSI) under a controlled atmosphere (<0.1 ppm O_2 and H_2O) and sealed until analysis. The analysis was carried out on ≈10 mg and under air (150 mL min^{-1}) at 10 °C min^{-1} from 0 to 425 °C. The weight accuracy was ±20 µg.

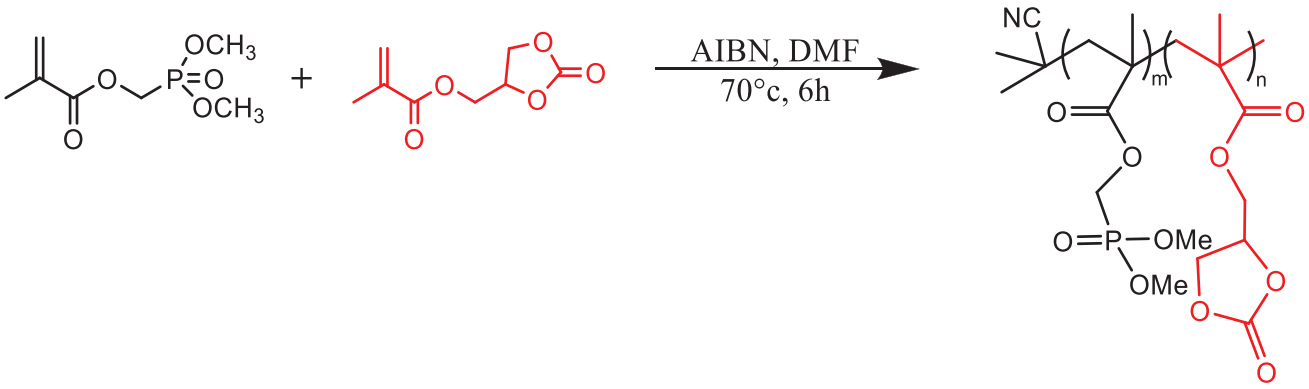

Scheme 3. Synthesis of poly(MAPC1-*r*-MAcy CB) copolymers.

2.6.4. Size Exclusion Chromatography (SEC)

Number averaged molar mass and dispersity ($\bar{M}n$ and Đ respectively) of polymers were measured on an Agilent system equipped with an Agilent 1200 pump, an Agilent differential refractometer, and two Polymer Standards Service Gram columns (100 and 1000 Å). DMF containing 2.5×10^{-3} mol l^{-1} of NH_4PF_6 was used as eluent with a flow rate of 1 mL min^{-1} and poly(methyl methacrylate) standards were used for calibration.

2.6.5. Scanning Electron Microscopy (SEM)

SEM analysis was conducted on a SEM Supra 55 equipped with a Gemini column (4 pA-20 nA probe current) using an Everhart-Thornley secondary electron detector with optically coupled photomultipliers. Energy-dispersive X-ray spectroscopy (EDX) images were recorded with an Oxford INCA-350 XMAX system. All scales were provided with a 10% precision.

2.6.6. Electrochemical Tests

All electrochemical tests were performed in an ITS from Bio-Logic which was a Peltier effect-based temperature control unit and was linked to a BioLogic VMP3 potentiostat. The samples were first sealed in a BioLogic CESH (Controlled Environment Sample Holder) in a glove box, consisting of two gold electrodes sandwiching the sample and having an internal PT-1000 probe to measure the sample temperature during testing. All tests were realized with a temperature accuracy of ±0.1 °C. The ionic conductivity was determined by impedance spectroscopy between 50 mHz and 1 MHz with a 10 mV amplitude and 8 points per decade, the samples were sandwiched between two 15.5 mm diameter SS disks before being placed in the CESH. The samples were equilibrated for 2 h before measurement. For linear sweep voltammetry (LSV), the samples (SPE membranes with LiTFSI) were sandwiched between a 15.5 mm diameter SS disk and a 15 mm diameter lithium disk (0.75 mm thickness) before being placed in the CESH. A 10 mV s^{-1} ramp was used starting from open circuit voltage (OCV) to 6 V or 0.5 V versus Li^+/Li.

Table 1. Molecular characteristic features of the synthesized copolymers and homopolymers.

Theoretical mol% ratio		Experimental mol% ratio		$\bar{M}n^{b)}$	Đ[b)]
MAPC1	MACyCB	MAPC1	MACyCB		
20	80	21.5	79.5	21×10^3 g mol^{-1}	2.9
50	50	47.3	53.7	16×10^3 g mol^{-1}	2.5
80	20	78	22	12×10^3 g mol^{-1}	2.1
100	0	100	0	61×10^3 g mol^{-1}	1.9
0	100	0	100	67×10^3 g mol^{-1}	2.6

[a)] Determined by ^{1}H NMR; [b)] Determined by SEC using poly(methyl methacrylate) calibration standards

3. Results and Discussion

3.1. Copolymerization of Dimethyl(methacryloyloxy) Methyl Phosphonate and 2-oxo-1,3-dioxolan-4-yl Methyl Methacrylate

A series of poly(MAPC1-*r*-MACyCB) random copolymers (**Scheme 3**) has been prepared by free radical copolymerization of dimethyl (methacryloyloxy) methyl phosphonate (MAPC1) and 2-oxo-1,3-dioxolan-4-yl methyl methacrylate (MACyCB) in DMF at 70 °C for 6 h using AIBN as initiator. The molar ratio of MACyCB has been varied from 20 to 80 mol% in order to investigate the effect of the copolymer composition on different properties such as ionic conductivity, the fire-retardant properties and the electrochemical stability. The molecular characteristic features of the investigated copolymers are summarized in **Table 1**.

They accordingly obtained copolymers have been analyzed by ^{1}H NMR at different conversions. In all cases, the copolymer composition as determined by ^{1}H NMR is similar to the monomer feed. Those results are pointed out towards a fully random distribution of the two comonomers in the copolymers. This is not a surprising result since both monomers are belonging to the methacrylate family and are not so different in terms of steric crowding. Therefore, similar reactivity ratios are expected for both monomers. The copolymerization reactions have been stopped at an 80 mol% conversion and SEC analysis has been

Table 2. Differential Scanning calorimetry and Thermal Gravimetric Analysis of homopolymers and copolymers with or without LiTFSI (at an equimolar ratio). *Polymer:LiTFSI ratio.

Sample composition	DSC (T_g,°C)		TGA (loss peaks,°C)	
	1 :0*	1 :1*	1 :0*	1 :1*
Poly(MAPC1)	58	2	327, 394	258, 338, 442
Poly(MACyCB)	43	−19	171, 283	228, 245, 310, 414
Poly(MAPC1) – Poly(MACyCB) 50–50	23	−20	176, 245, 325; 396	252, 272, 330, 443
Poly(MAPC1-r-MACyCB) 50–50	65	≤−70	333	262, 303, 455

performed to obtain an estimation of the apparent molar mass and of the dispersity (*Đ*) of the synthesized copolymers (Table 1). Homopolymers of MACyCB and MAPC1 have been also synthesized using the same protocol and will be further mixed in molar ratios identical to the molar compositions of the random copolymers. The properties of the mixtures of poly(MACyCB) and poly(MAPC1) homopolymers will be further compared to those of poly(MAPC1-*r*-MACyCB) copolymers of similar molar compositions.

3.2. Preparation of Solid Polymer Electrolytes

The SPE membranes were prepared by a drop-casting method. More precisely, a solution consisting of poly(MAPC1-*r*-MACyCB) copolymer or a mix of poly(MACyCB) and poly(MAPC1) homopolymers, lithium bis(trifluoromethanesulfonyl)imide (LiTFSI) and acetonitrile have been cast on a SS disk or in a PTFE mold and then dried under vacuum at 40 °C during 24 h to ensure complete acetonitrile removal. In addition to the variation of the copolymer composition and the evaluation of the corresponding homopolymer mixtures, the amount of loaded LiTFSI salt has also been changed from monomer units:LiTFSI molar ratios of 5:1, 1:1, and 1:2, respectively. As a rule, the higher the loading in LiTFSI, the less brittle the SPE membranes. This observation could be correlated with the decreased glass transition (T_g) of the SPE when the amount of LiTFSI is increased (see next section for T_g measurements). In sharp contrast to SPE membranes prepared in PTFE molds, it was hard to peel off the sample prepared on SS disks, most probably because of the interactions of phosphonate moieties with the metal surface. Finally, it is worth mentioning that all the prepared SPE membranes were looking macroscopically homogeneous and did not reveal the presence of insolubilized LiTFSI domains even with the highest salt loading (1:2) corresponding to ≈75 wt.% of lithium salt in the membrane. Further information about the possible presence of LiTFSI domains will be provided in the next section by scanning electron microscopy (SEM).

3.3. Thermal Properties

DSC has been used to determine the T_g of the investigated SPEs (**Table 2**). In the context of SPEs, this temperature is very important because the ionic conductivity should be higher above T_g (better segmental mobility) than below. Furthermore, particles or salt in the polymer matrix often act as plasticizers which will influence the T_g, and, depending on the interactions with the polymer chains, will increase or not the ionic conductivity.[48,49] The initial T_gs of poly(MAPC1) and poly(MACyCB) homopolymers are 58 °C and 43 °C, respectively. However, the introduction of LiTFSI at a 1:1 molar ratio decreases both T_gs until 2 °C for poly(MAPC1) and −19 °C for poly(MACyCB) (Figures S6 and S7, Supporting Information), confirming the plasticizing effect of LiTFSI on both homopolymers. Moreover, a mixture of 50 mol% of each homopolymer, without LiTFSI, leads to only one T_g observable at the second heat, around 23°C which indicates a good miscibility between both homopolymers,[50] the same phenomenon is observed when LiTFSI is added, but with a lower T_g (−20 °C for an equimolar ratio of polymer units:LiTFSI, Figure S8). Lastly, the poly(MAPC1-*r*-MACyCB) random copolymer with 50 mol% of MAPC1 units shows one T_g of 65 °C without LiTFSI and around −70 °C with a 1:1 LiTFSI molar ratio (Figure S9, Supporting Information), nevertheless this last T_g is not accurately measured because it was in the limit range analysis for our DSC measurement. We can thus conclude that the mixtures of MACyCB and MAPC1 are miscible in the homopolymer or copolymer configuration. Besides, the T_g seems to be more influenced by the addition of LiTFSI in the copolymer system.

TGA has been used to evaluate the thermal stability of the investigated polymers (Table 2). We have defined thermal stability as the temperature at which the sample has a maximum in the weight loss rate, calculated by the derivation of weight loss as a function of temperature. We have investigated both homopolymers (poly(MAPC1) and poly(MACyCB)), as well as an equimolar homopolymer mix and a copolymer containing an equimolar amount of both units (Figure S10) with or without LiTFSI. The different values corresponding to the weight loss derived maxima (**Figure 1**) are reported in Table 2. The lowest thermal stability is observed for pol(MACyCB) without LiTFSI, with a first peak at 171 °C whereas poly(MAPC1) is stable until 327 °C without LiTFSI. As expected, the homopolymer mixture gave results similar to the gathering of both homopolymer thermal stability, but the copolymer has only one main thermal degradation, around 333 °C, which corresponds to the main poly(MAPC1) degradation. This suggests that the copolymer structure, without lithium salt, can help to increase the thermal stability of MACyCB units. When LiTFSI was added to the different polymer systems, a degradation around 440 °C was observed for all samples, which corresponds to LiTFSI degradation.[51] Moreover, the thermal stability of the LiTFSI-loaded copolymer system is again higher than homopolymers-based ones. Regarding residual weight

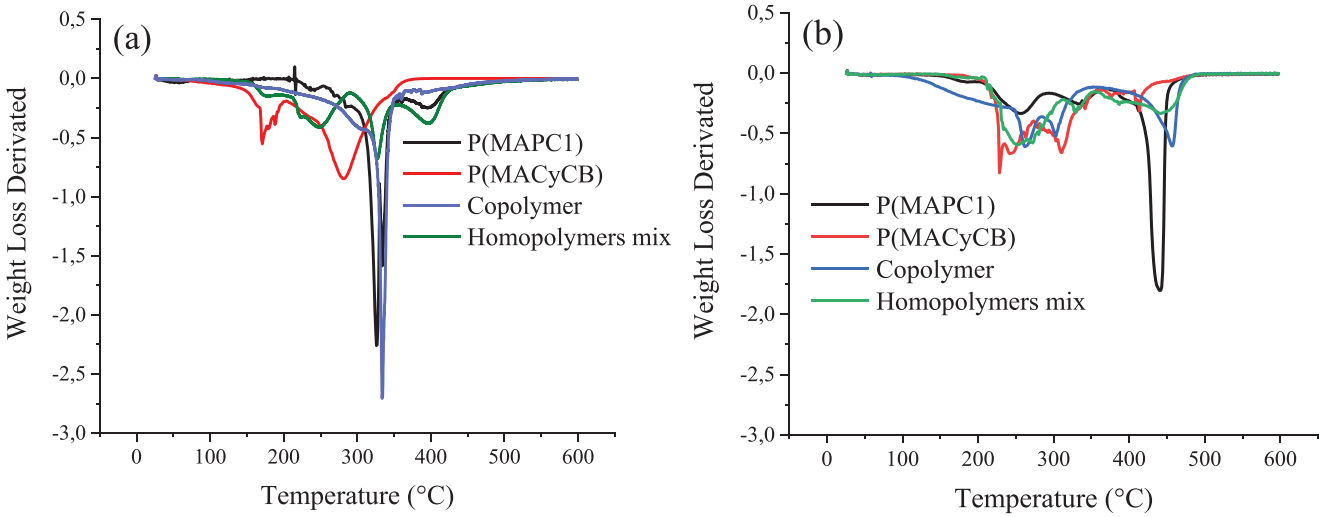

Figure 1. Derived weight loss from thermogravimetric analysis of poly(MACyCB) (red), poly(MAPC1) (black), an equimolar amount of MACyCB and MAPC1 units in a random copolymer (blue) or homopolymers mix (green), a) without LiTFSI, b) with a monomer units:LiTFSI molar ratio of 1:1.

(Figure S10, Supporting Information) without LiTFSI, there is no significant difference between all samples (≈20%), which can be explained by the fact that all investigated polymers share the same backbone based on methyl methacrylate units. To conclude this part, the thermal stability of the investigated polymer systems is high enough in all cases for further use as SPEs in batteries.

3.4. Electrochemical Stability

The electrochemical stability of the investigated (co)polymers has been studied by linear sweep voltammetry (LSV) in a Li|SPE|SS configuration and is defined as the voltage at which a positive (oxidation) or negative (reduction) inflexion is observed in the curve. It is depicted in **Figure 2** for the poly(MAPC1) and poly(MACyCB) homopolymers and the 50:50 mol mol^{-1} corresponding copolymers, all loaded with LiTFSI at a molar ratio of 1:1. Clearly, the phosphonate-containing polymer poly(MAPC1) is stable at low voltage (1.5 V vs Li$^+$/Li) as well as at high voltage (above 5 V vs Li$^+$/Li) allowing a possible use in solid-state batteries consisting of lithium metal at the anode and high voltage materials as cathode. In contrast, the cyclocarbonate-containing poly(MACyCB) polymer is only stable between 1.8 and 3.5 V vs Li$^+$/Li and reach a maximum around 4.1 V, in agreement with previously reported electrochemical stability for carbonate-containing polymer electrolytes.[52–54] As expected, the electrochemical stability of poly(MAPC1-*r*-MACyCB) based electrolytes is limited by the MACyCB component, with a similar cathodic stability compared to poly(MACyCB) but in two steps: a first small peak around 2 V then a continuous reduction until 0.5 V. Regarding the anodic curve, we observe a better stability than poly(MACyCB), with a small peak around 4.5 V and then a continuous oxidation until 5.5 V. This means the presence of MAPC1 in the copolymer helps to increase the MACyCB electrochemical stability, which can be due to an electrochemical stabilization of MACyCB as a result of interaction with MAPC1.

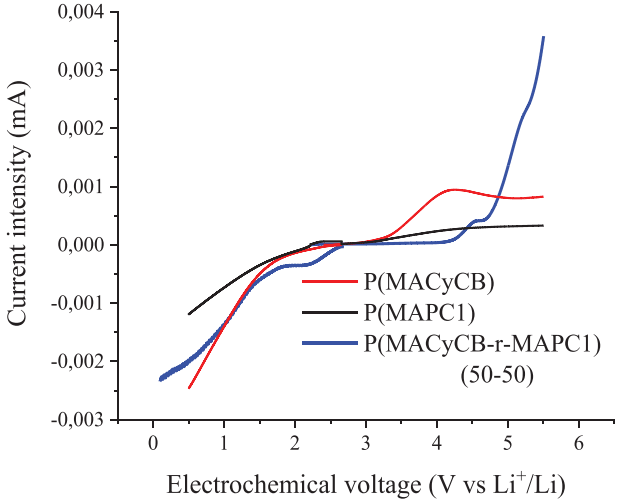

Figure 2. Electrochemical stability between 0.5 and 5.5 V versus Li$^+$/Li of poly(MAPC1) (black), poly(MACyCB) (red) and poly(MAPC1-*r*-MACyCB) (blue) (50–50), with a 1:1 molar ratio of LiTFSI.

3.5. Ionic Conductivity Measurements

Ionic conductivity measurements have been systematically performed on the investigated samples in order to highlight the effect of the composition and of the structure of the polymer component as well as the lithium salt loading on the conductivity values. All tests have been performed from 60 to 20 °C and ionic conductivity (σ in S cm^{-1}) has been calculated according to Equation 1.

$$\sigma = \frac{t}{R \times S} \quad (1)$$

with t = thickness (in cm), R = resistance of sample (Ω) and S = surface of samples (cm^2). R has been measured by potentiostatic electrochemical impedance spectroscopy (PEIS) between 1 MHz

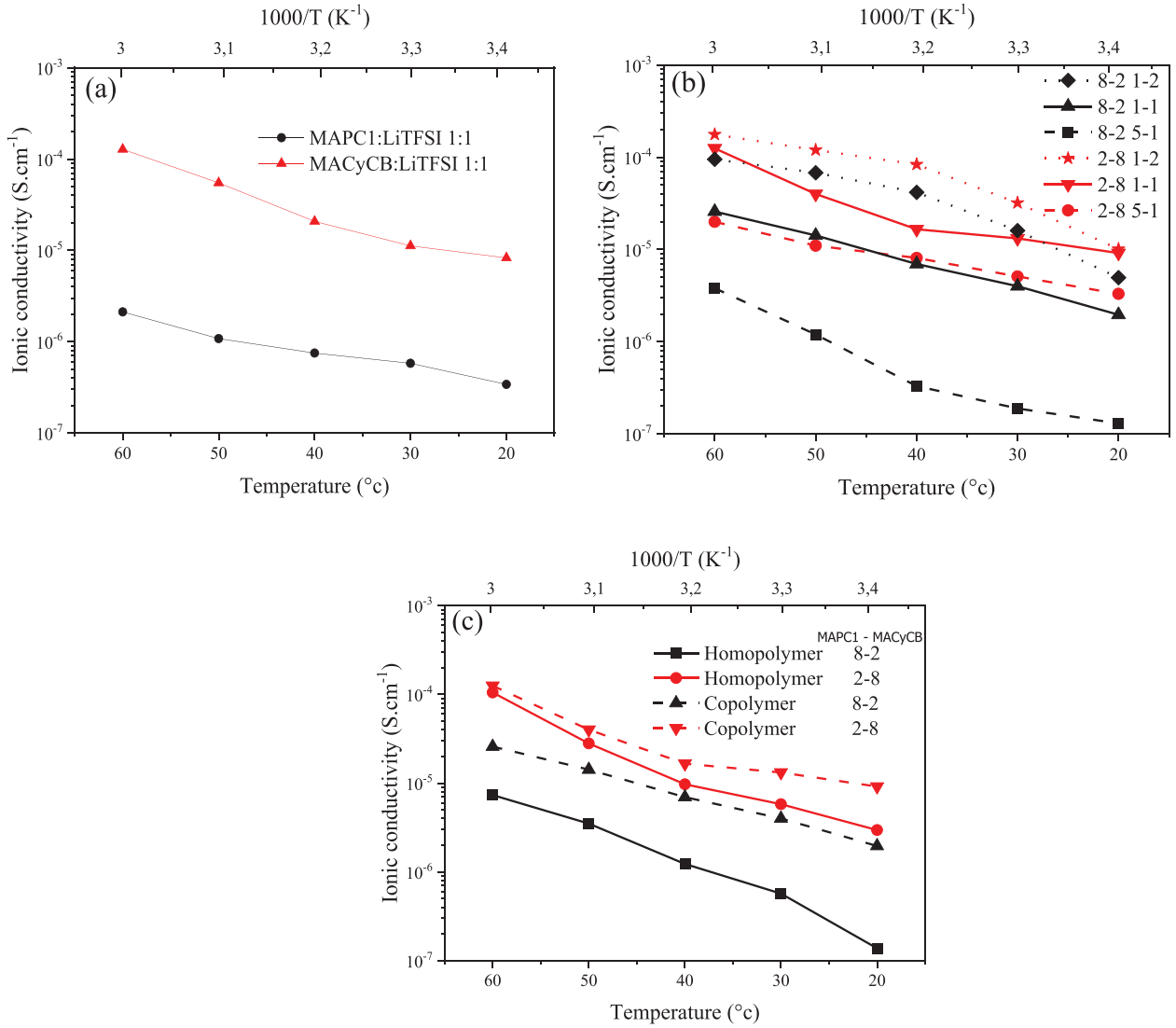

Figure 3. Ionic conductivity measurements of as a function of temperature for a) poly(MAPC1) (black) and poly(MACyCB) (red) homopolymers with a monomer units:LiTFSI 1:1 molar ratio; b) two different poly(MAPC1-*r*-MACyCB) copolymer-based electrolytes with 8–2 (black) and 2–8 (red) molar compositions (see Table 1) with different monomer units:LiTFSI molar ratios of 5:1 (dash lines), 1:1 (straight lines) and 1:2 (dot lines); c) comparison between poly(MAPC1-*r*-MACyCB) copolymers or mixtures of homopolymers electrolytes with similar molar compositions and with monomer units:LiTFSI 1:1 molar ratio.

and 50 mHz and *t* is the thickness measured after the complete analysis cycle from 60 to 20 °C.

In the first step, ionic conductivity of poly(MACyCB) and poly(MAPC1) homopolymers with a LiTFSI molar ratio of 1:1 have been measured (**Figure 3**a). The ionic conductivity of poly(MACyCB) is ≈10^{-5} S cm^{-1} at room temperature and is above 10^{-4} S cm^{-1} at 60 °C. Those values correspond to the state-of-the-art for SPEs containing carbonate units reported by Mercerreyes[55–57] and Brandell.[58–60] In the case of poly(MAPC1), the ionic conductivity was 3.4 × 10^{-7} S cm^{-1} at room temperature and hardly reached values above 10^{-6} S cm^{-1} at 60 °C, in agreement with our recent study on phosphonate-based SPEs.[42] The use of the phosphonate polymer is thus motivated by its fire-retardant properties rather than ionic conducting properties.

To further illustrate this point, the ionic conductivity of poly(MAPC1-*r*-MACyCB)-based SPEs has been measured as shown in Figure 3b. Two compositions have been examined: one MAPC1-rich (the 8-2 sample in Figure 3b with 80 mol% of MAPC1 in the poly(MAPC1-*r*-MACyCB) copolymer) and one MACyCB-rich (the 2–8 sample in Figure 3b with 80 mol% of MACyCB in the poly(MAPC1-*r*-MACyCB) copolymer). As expected, ionic conductivity is much lower for the 8–2 samples compared to the 2–8 ones at the same salt loading (Figure 3b), in agreement with the data obtained on the poly(MACyCB) and poly(MAPC1) homopolymers.

The effect of the salt loading on the ionic conductivity has been evaluated and is shown in Figure 3b for the 2–8 and 8–2 samples. More precisely, salt loadings corresponding to monomer units:LiTFSI molar ratios of 5:1, 1:1, and 1:2 have been inves-

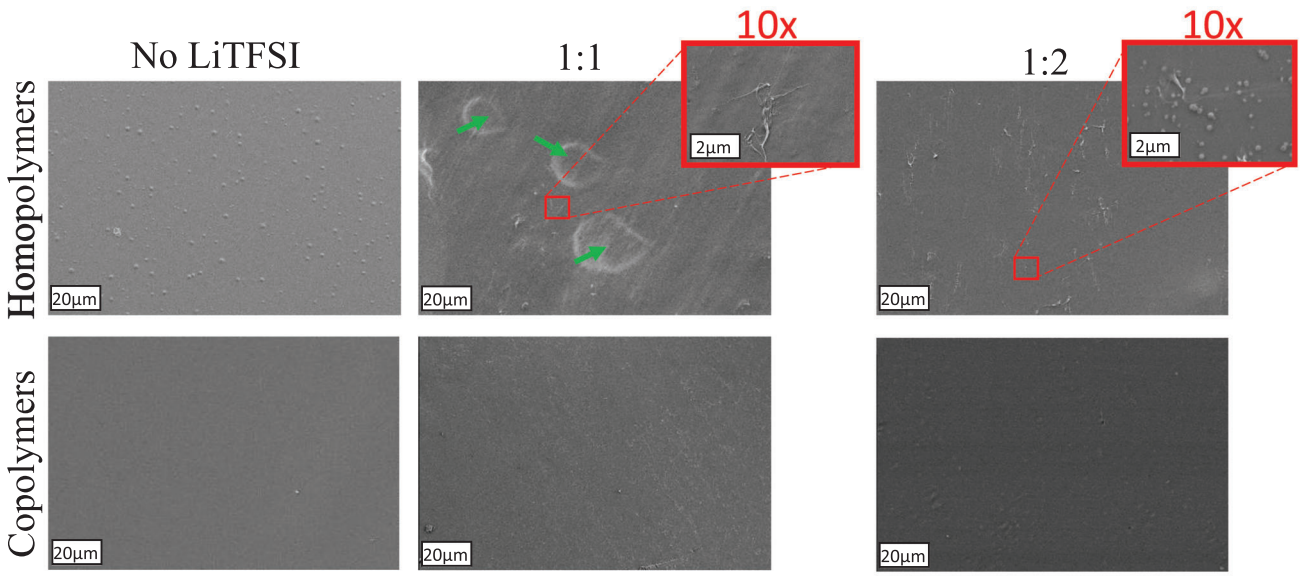

Figure 4. Top: SEM pictures of 50:50 mol mol^{-1} mixtures of poly(MAPC1) and poly(MACyCB) homopolymers without LiTFSI or with monomer units:LiTFSI molar ratios of 1:1 and 1:2. Down: SEM pictures of poly(MAPC1-*r*-MACyCB) 5–5 copolymer without LiTFSI or with monomer units:LiTFSI molar ratios of 1:1 and 1:2. The red frames represent a 10x zoom of the SEM image to highlight aggregates. Green arrows show the regions where the chemical composition is different from the rest of the sample (see Figure S11, Supporting Information). The white bar in the down-left corner corresponds to 20 µm.

tigated. As a rule, the higher the LiTFSI loading, the higher the ionic conductivity. Nevertheless, the added lithium salt acts as a plasticizer (see previously discussed DSC results) and, in the case of the SPEs with the highest salt content (monomer units:LiTFSI 1:2 mol mol^{-1}), the obtained electrolyte is so soft that it easily leads to short-circuiting during the measurements at 60 °C or higher temperature. Therefore, the monomer units:LiTFSI ratio of 1:1 mol mol^{-1} has been selected as the best candidate for the next investigations.

As a last step, the impact on the ionic conductivity of the random copolymer architecture compared to a mixture of the corresponding homopolymers, both characterized by the same molar ratio of MACyCB and MAPC1 and the same monomer units:LiTFSI ratio of 1:1 mol mol^{-1}, and is shown in Figure 3c. Again, the SPEs containing a major part of MACyCB units displays a higher ionic conductivity. Moreover, it is interesting to point out that the poly(MAPC1-*r*-MACyCB) random copolymer-based SPEs show better ionic conductivity than the corresponding poly(MACyCB) and poly(MAPC1) homopolymers mixtures, all the other parameters being constant (Figure 3c). This means that having the phosphonate units randomLy distributed on the same chain as cyclocarbonate groups, impacts less the ionic conductivity originating from the cyclocarbonates. In this respect, a copolymer having 80 mol% of MACyCB and 20 mol% of MAPC1 is reaching almost the same ionic conductivity as the poly(MACyCB) homopolymer and have an ionic conductivity three times bigger than the corresponding homopolymer mix. This shows the possibility to largely improve ionic conductivity just by changing the polymer conformation and having the possibility to add a fire-retardant in the structure without significant impact on it.

3.6. Morphology of Solid Polymer Electrolytes

SEM has been used to compare the morphologies of SPEs obtained from poly(MAPC1-*r*-MACyCB) copolymers and mixtures of poly(MACyCB) and poly(MAPC1) homopolymers. **Figure 4** shows the results obtained for those systems with a MACyCB:MAPC1 50:50 molar ratio and with various monomer units:LiTFSI molar ratios of 1:0, 1:1 and 1:2.

The SPE membranes obtained from homopolymers mixtures without added LiTFSI revealed some bubbles on their surfaces while few aggregates are observed for the monomer units:LiTFSI molar ratio of 1:1 and more aggregates for the 1:2 ratio (Figure 4). Those aggregates could be ascribed to LiTFSI salt not dissolved in the polymer matrix or to sample morphological defects, which is more likely since back-scattered electron detection gave smooth images, meaning no significant atomic number difference between those aggregates and the rest of the sample (Figure S12, Supporting Information). These bubbles are mostly visible in the sample without LiTFSI, which could be tentatively explained by a lower solubility of both homopolymers in the absence of lithium salt. This could lead to the aggregation of homopolymers particles which can explain why no change in atomic number was observed with back-scattered electron detection. Moreover, the SEM images also reveal some micrometer size domains in the polymer matrix. Those are clearly visible for the homopolymer mixture with a monomer units:LiTFSI molar ratio of 1:1 and have been spotted with green arrows in Figure 4. In order to obtain information about the chemical composition of those domains, energy dispersive X-Ray (EDX) analysis was conducted on those specific areas (Figure S11, Supporting Information) and reveal that they are characterized by the same fluorine and sulfur content but a

lower phosphorus content that the rest of the sample. Those observations give credit to a homogeneous dispersion of the LiTFSI salt within the whole sample except for the few LiTFSI aggregates, and to a microphase separation between both homopolymers as highlighted by the observation of poly(MACyCB)-rich domains in Figure 4. This is the contrary of DSC results on homopolymer mixtures which show only one T_g at the second heating cycle. This can be explained by a lack of homogeneity in SEM samples, which have not been melted but drop casting, also the accuracy of DSC measurement could not be enough to differentiate both T_gs in a homopolymer mix with lithium salt, since they are very similar as shown before.

In contrast, no phase separation is observed for membranes prepared from poly(MAPC1-*r*-MACyCB) copolymers (Figure 4, bottom) and LiTFSI aggregates are hardly observed. Those observations give credit to the higher ionic conductivity observed for poly(MAPC1-r-MACyCB)-based SPEs compared to those prepared from the corresponding homopolymer mixtures (Figure 3).

3.7. Flammability Tests

The main role of phosphonate in our system is to bring a fire-retardant property to the SPE. To prove this concept, fire resistance tests have been performed on SPE membranes prepared from polymers with a monomer units:LiTFSI molar ratio of 1:1. Those membranes have been exposed for 2 s in a Bunsen flame using mains gas (mainly methane) and then removed from the flame to observe if the sample goes on burning or not (**Figure 5**).

As a reference, a PEO SPE has been prepared (Figures 5a-c). The PEO SPE membranes burns easily and almost all the membrane is consumed after flame exposition, which is similar for the pure poly(MACyCB) SPE membrane (Figures 5d-f). A fire test on a pure poly(MAPC1) SPE membrane could not be performed, because it is too brittle to obtain a self-standing membrane. Nevertheless, membranes prepared from mixtures of poly(MACyCB) and poly(MAPC1) homopolymers show good fire-retardant properties. Indeed, the SPE membrane obtained from the poly(MAPC1)-poly(MACyCB) (80–20 mol%) mixture and containing a majority of phosphonate groups (Figures 5j–l) does not burn at all, even if it is placed several times again in the flame. This demonstrates that MAPC1 units really bring some fire-retardant properties to SPEs. More interesting is the result obtained for the poly(MAPC1)-poly(MACyCB) (80–20 mol%) mixture with a majority of cyclocarbonate units, that does not burn after the Bunsen exposition but rather melts (Figures 5g–i). This means that a 20 mol% content of phosphonate units in the SPE is enough to bring fire retardant property while not compromising too much ionic conductivity. We can conclude that MAPC1 is a promising monomer unit for future safer SPEs.

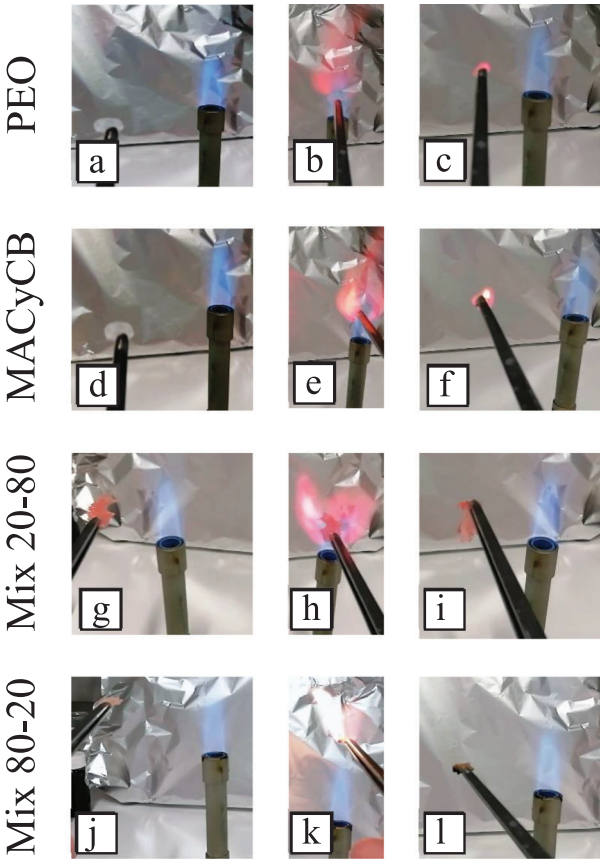

Figure 5. Flammability tests for SPE membranes (all loaded with a monomer units:LiTFSI molar ratio of 1:1) based on a a—c) PEO reference, d—f) poly(MACyCB) homopolymer, g—i) a mixture of poly(MAPC1) and poly(MACyCB) homopolymers with 20–80 mol% respectively, j—l) and a mix of poly(MAPC1)-poly(MACyCB) homopolymers with 80–20 mol% respectively. The first picture is the film before the test (a,d,g,j), the second picture is in the flame for 2 s (b,e,h,k) and the third picture is 2 s after having been removed from the flame (c,f,i,l).

4. Conclusion

In this work, we report on an innovative SPE system based on two monomer units, a phosphonate (MAPC1) and a cyclocarbonate (MACyCB). MACyCB is the most interesting component regarding ionic conductivity, whatever the LiTFSI content or the formulation (in copolymer or homopolymer mixture). This can be explained by a better lithium salt solubility as well as a lower glass transition temperature compared to MAPC1. Nevertheless, MAPC1 is an interesting unit to add in a SPE, together with MACyCB, because it retains the fire-retardant property of phosphonate while not impacting the ionic conductivity of MACyCB when present at a 20 mol% content. The SPE membranes based on the copolymer system shows a more homogeneous dispersion of components and a better LiTFSI solubilization than the corresponding homopolymer-based SPEs, leading to better ionic conductivity based on the polymer architecture more than in the chemical composition. Finally, some preliminary cycling experiments (Figure S13, Supporting Information) have revealed an acceptable rate capability with LFP, with 96 mAh g^{-1} after 150 cycles corresponding to only 8% capacity fading at 20 °C. This innovative system should be further investigated in Li metal batteries in order to demonstrate its full potential.

Supporting Information

Supporting Information is available from the Wiley Online Library or from the author.

Acknowledgements

The author is grateful to INNOVIRIS for an APPLIED Ph.D. grant and to UCL and SOLVAY S.A. for the Ph.D. position and laboratories access.

Conflict of Interest

The authors declare no conflict of interest.

Data Availability Statement

The data that support the findings of this study are available from the corresponding author upon reasonable request.

Keywords

cyclocarbonate, fire-retardant properties, phosphonate, radical polymerization, solid polymer electrolytes, solid-state batteries

Received: May 11, 2022
Revised: August 11, 2022
Published online: September 4, 2022

[1] N. Rietmann, B. Hügler, T. Lieven, *J. Cleaner Prod.* 121038, **2020**, *261*.
[2] T. P. Narins, *Extr. Ind. Soc.* **2017**, *4*, 321.
[3] Y. Chen, Y. Kang, Y. Zhao, L. Wang, J. Liu, Y. Li, Z. Liang, X. He, X. Li, N. Tavajohi, B. Li, *J. Energy Chem.* **2021**, *59*, 83.
[4] A. Ahmad, Z. A. Khan, M. Saad Alam, S. Khateeb, *Smart Sci.* **2017**, *6*, 36.
[5] J. Janek, W. G. Zeier, *Nat. Energy* **2016**, *1*, 16141.
[6] W. Xu, J. Wang, F. Ding, X. Chen, E. Nasybulin, Y. Zhang, J.-G. Zhang, *Energy Environ. Sci.* **2014**, *7*, 513.
[7] D. T. Hallinan, N. P. Balsara, *Annu. Rev. Mater. Res.* **2013**, *43*, 503.
[8] S. Ohta, T. Kobayashi, J. Seki, T. Asaoka, *J. Power Sources* **2012**, *202*, 332.
[9] J. Li, C. Ma, M. Chi, C. Liang, N. J. Dudney, *Adv. Energy Mater.* **2015**, *5*, 1401408.
[10] W. D. Richards, L. J. Miara, Y. Wang, J. C. Kim, G. Ceder, *Chem. Mater.* **2015**, *28*, 266.
[11] A. C. Luntz, J. Voss, K. Reuter, *J. Phys. Chem. Lett.* **2015**, *6*, 4599.
[12] W. H. Meyer, *Adv. Mater.* **1998**, *10*, 439.
[13] C. Monroe, J. Newman, *J. Electrochem. Soc.* **2005**, *152*, A396.
[14] G. M. Stone, S. A. Mullin, A. A. Teran, D. T. Hallinan, A. M. Minor, A. Hexemer, N. P. Balsara, *J. Electrochem. Soc.* **2012**, *159*, A222.
[15] Y. Li, K. Leung, Y. Qi, *Acc. Chem. Res.* **2016**, *49*, 2363.
[16] A. Manthiram, X. Yu, S. Wang, *Nat. Rev. Mater.* **2017**, *2*, 16103.
[17] M. Armand, *Solid State Ionics* **1994**, *69*, 309.
[18] D. E. Fenton, J. M. Parker, P. V. Wright, *Polymer* **1973**, *14*, 589.
[19] W. Gorecki, M. Jeannin, E. Belorizky, C. Roux, M. Armand, *J. Phys.: Condens. Matter* **1995**, *7*, 6823.
[20] A. Manuel Stephan, K. S. Nahm, *Polymer* **2006**, *47*, 5952.
[21] Y. Wang, W.-H. Zhong, *ChemElectroChem* **2015**, *2*, 22.
[22] F. Croce, G. B. Appetecchi, L. Persi, B. Scrosati, *Nature* **1998**, *394*, 456.
[23] J. Zagórski, J. M. López del Amo, M. J. Cordill, F. Aguesse, L. Buannic, A. Llordés, *ACS Appl. Energy Mater.* **2019**, *2*, 1734.
[24] F. Müller-Plathe, W. F. Van Gunsteren, *J. Chem. Phys.* **1995**, *103*, 4745.
[25] M. Armand, *Adv. Mater.* **1990**, *2*, 278.
[26] V. Bocharova, A. P. Sokolov, *Macromolecules* **2020**, *53*, 4141.
[27] M. Yuan, J. Erdman, C. Tang, H. Ardebili, *RSC Adv.* **2014**, *4*, 59637.
[28] J.-C. Daigle, A. Vijh, P. Hovington, C. Gagnon, J. Hamel-Pâquet, S. Verreault, N. Turcotte, D. Clément, A. Guerfi, K. Zaghib, *J. Power Sources* **2015**, *279*, 372.
[29] T. Okumura, S. Nishimura, *Solid State Ionics* **2014**, *267*, 68.
[30] J. Zhang, J. Zhao, L. Yue, Q. Wang, J. Chai, Z. Liu, X. Zhou, H. Li, Y. Guo, G. Cui, L. Chen, *Adv. Energy Mater.* **2015**, *5*, 1501082.
[31] F. Boujioui, H. Damerow, F. Zhuge, J. F. Gohy, *Macromol. Chem. Phys.* **2020**, *221*, 1900556.
[32] F. Boujioui, F. Zhuge, H. Damerow, M. Wehbi, B. Améduri, J.-F. Gohy, *J. Mater. Chem. A* **2018**, *6*, 8514.
[33] A. F. Zonouz, *Anal. Bioanal. Electrochem.* **2018**, *10*, 1053.
[34] L. D. Quin, *A Guide to Organophosphorus Chemistry*, John Wiley & Sons, New York, USA **2000**, Chapter 2, 10, 11.
[35] D. E. C. Corbridge, *Phosphorus Chemistry, Biochemistry and Technology*, CRC Press, Boca Raton, USA **2013**.
[36] B. Chaloner-Gill, (Valence Technology Inc.), US Patent 5393621, **1995**.
[37] J. Zheng, X. Liu, Y. Duan, L. Chen, X. Zhang, X. Feng, W. Chen, Y. Zhao, *J. Membr. Sci.* **2019**, *583*, 163.
[38] J. Zheng, Y. Zhao, X. Feng, W. Chen, Y. Zhao, *J. Mater. Chem. A* **2018**, *6*, 6559.
[39] J. Zheng, Y. Yang, W. Li, X. Feng, W. Chen, Y. Zhao, *J. Mater. Chem. A* **2020**, *8*, 22962.
[40] H. Jia, H. Onishi, R. Wagner, M. Winter, I. Cekic-Laskovic, *ACS Appl. Mater. Interfaces* **2018**, *10*, 42348.
[41] S. Popa, S. Iliescu, G. Ilia, N. Plesu, A. Popa, A. Visa, L. Macarie, *Eur. Polym. J.* **2017**, *94*, 286.
[42] L. Bai, M. Webhi, G. Dolphijn, B. Améduri, J. F. Gohy, *Macromol. Chem. Phys.* **2020**, *222*, 2000389.
[43] H. Li, Y. Kuai, J. Yang, S.-I. Hirano, Y. Nuli, J. Wang, *J. Energy Chem.* **2022**, *65*, 616.
[44] J. L. Olmedo-Martínez, L. Meabe, R. Riva, G. Guzmán-González, L. Porcarelli, M. Forsyth, A. Mugica, I. Calafel, A. J. Müller, P. Lecomte, C. Jérôme, D. Mecerreyes, *Polym. Chem.* **2021**, *12*, 3441.
[45] Z. El Asri, K. Chougrani, C. Negrell-Guirao, G. David, B. Boutevin, C.ã©D. Loubat, *J. Polym. Sci., Part A: Polym. Chem.* **2008**, *46*, 4794.
[46] B. Canniccioni, S. Monge, G. David, J.-J. Robin, *Polym. Chem.* **2013**, *4*, 3676.
[47] M. Yoshikawa, N. Hotta, J. Kyoumura, Y. Osagawa, T. Aoki, *Sens. Actuators, B* **2005**, *104*, 282.
[48] M. U. X. Helan Flora, S. Rajendran, *Int. J. Electrochem. Sci.* **2012**, *7*, 7451.
[49] J. Cruickshank, H. V. S. A. Hubbard, N. Boden, I. M. Ward, *Polymer* **1995**, *36*, 3779.
[50] M. Aubin, R. E. Prud'homme, *Macromolecules* **2002**, *21*, 2945.
[51] Z. Lu, L.i Yang, Y. Guo, *J. Power Sources* **2006**, *156*, 555.
[52] N.-S. Choi, S.-W. Ryu, J.-K. Park, *Electrochim. Acta* **2008**, *53*, 6575.
[53] K. Kimura, Y. Tominaga, *ChemElectroChem* **2018**, *5*, 4008.
[54] G. Yan, D. Alves-Dalla-Corte, W. Yin, N. Madern, G. Gachot, J.-M. Tarascon, *J. Electrochem. Soc.* **2018**, *165*, A1222.
[55] L. Meabe, N. Goujon, C. Li, M. Armand, M. Forsyth, D. Mecerreyes, *Batteries Supercaps* **2019**, *3*, 68.
[56] P. Sutton, M. Airoldi, L. Porcarelli, J. L. Olmedo-Martinez, C. Mugemana, N. Bruns, D. Mecerreyes, U. Steiner, I. Gunkel, *Polymers* **2020**, *12*, 595.
[57] L. Meabe, T. V. Huynh, D. Mantione, L. Porcarelli, C. Li, L. A. O'dell, H. Sardon, M. Armand, M. Forsyth, D. Mecerreyes, *Electrochim. Acta* **2019**, *302*, 414.
[58] J. Mindemark, B. Sun, E. Törmä, D. Brandell, *J. Power Sources* **2015**, *298*, 166.
[59] J. Mindemark, E. Törmä, B. Sun, D. Brandell, *Polymer* **2015**, *63*, 91.
[60] J. Mindemark, L. Imholt, J. Montero, D. Brandell, *J. Polym. Sci., Part A: Polym. Chem.* **2016**, *54*, 2128.